

IMPACT OF SPECIFIC METALLURGICAL IMPURITIES IN SILICON FEEDSTOCK ON SOLAR CELL EFFICIENCY, AND POTENTIAL BENEFITS OF N-TYPE DOPING.

L.J. Geerligs

Energy research Centre of the Netherlands ECN, Petten, Netherlands

ABSTRACT: This paper gives an overview of work in a series of European projects (SOLSILC, SPURT, SISI, and FOXY) on p- and n-type mc-Si ingots doped with C, Al, Ti, and Fe. The aim of that work is to understand how impurities affect cell efficiency, and to determine which levels of impurities can be tolerated in silicon feedstock. A model is described and demonstrated for the dependence of cell efficiency on concentration of contaminants such as Ti and Al. The n-type silicon appears to be more tolerant than p-type to these impurities, at least from the point of view of the recombination lifetime. This is consistent with theoretical consideration of recombination activity of point defects. In addition we discuss recombination activity of extended defects in n- and p-type mc-Si wafers grown without artificial contamination of the feedstock. Both types show significant recombination activity of extended defects. Also the evolution of recombination at the extended defects after gettering and hydrogenation of the wafer is qualitatively similar for n- and p-type wafers. We discuss a simple model for the recombination activity of precipitates of impurity silicides, showing that indeed for extended defects it could be that there is no advantage of n-type doping.

1 INTRODUCTION

Soon, solar grade silicon will be available for PV. One potential source of solar grade silicon is from the direct carbothermic reduction of quartz and carbon. New solar grade silicon might contain significantly higher fractions of impurities. As one of the tasks in a series of European projects (SOLSILC, SPURT, SISI, and FOXY), we therefore investigated the impact of such impurities on cell efficiency, using ingots which were purposely contaminated with the impurities. The investigated impurities, Fe, Ti, Al, and C, were chosen because of their foreseen relevance in silicon produced by a metallurgical process [1,2,3]. They are also important for today's multicrystalline silicon (mc-Si) wafers because they are present in crucible materials and ingot growth equipment.

There have been several efforts in the past on specifically studying individual impurities in silicon feedstock [4,5,6]. Ref. 4 involved Cz-growth rather than mc-Si ingot growth. Ref. 5 involved mc-Si ingots, but did not include Ti. Both did not use a modern cell process with $\text{SiN}_x\text{:H}$ antireflection coating. Therefore we find it appropriate to revisit the question of feedstock specification with purposely contaminated ingots.

It is known that the interstitial point defects Ti, V, Cr, Mo, Fe in silicon capture electrons much more effectively than holes [7]. Therefore these defects are expected to be less detrimental for carrier recombination lifetime in n-type silicon, where holes are the less abundant (minority) carriers, than in p-type silicon, where electrons are the minority carriers. The same effect applies to the aluminium-related defect observed in Cz wafers [8]. This asymmetry in capture cross sections also causes a different sensitivity to wafer resistivity. Recombination lifetime in n-type wafers due to these defects is practically insensitive to resistivity, while in p-type wafers it can show a strong decrease with decreasing resistivity.

Thus, a second aim of this work is to determine whether high concentrations of impurities (especially Fe, Ti, Al) can be tolerated better in n-type silicon than in p-type silicon. In relation to this, it is possible that for n-

base cells a lower resistivity is allowed than is commonly allowed for p-base wafers, thus enhancing the cell V_{oc} and efficiency. For n-type silicon, this paper presents first results mainly for silicon contaminated with a mix of the impurities. Most of the results presented here may be found in [9].

Many studies have been performed on the relation between impurities and recombination and cell efficiency in "normal" (not purposely contaminated) mc-Si materials. The interaction of the impurities with extended crystal defects is of particular importance. Detailed studies of this kind will be presented by others at this conference [10]. In this paper we will shortly discuss whether a clear difference in recombination activity of extended defects between n- and p-type doped mc-Si is observed, and whether such a difference should in fact be expected at all.

2 ARTIFICIALLY CONTAMINATED INGOTS

2.1 Experimental ingots

Two p-type and two n-type ingots were grown with a mix of impurities. Additional p-type ingots were grown with the individual impurity Al or Ti.

The silicon was crystallised by directional solidification into a 12 kg ingot, wafered, and processed to cells by industrial cell processing (experimental cell processing based on industrial techniques, for the case of n-type base).

Table I: List of ingots and concentration of impurities in the feedstock. Impurity levels in ppmw (parts-per-million by weight).

ingot	type	ρ Ωcm	impurities		
			Al	Ti	Fe
p-5Al	p	1	5		
p-10Ti	p	2		10	
p-10Ti16Fe-A	p	2		10	16
p-10Ti16Fe-B	p	2		10	16
n-5Al1Ti3Fe	n	0.1	5	1	3
n-40Al10Ti70Fe	n	0.2	40±20	10±5	70±30

The p-type ingots were doped with boron to result in a base resistivity of approx. 1.5 Ωcm . The n-type ingots so far were doped with phosphorous to a much lower base resistivity of around 0.1 Ωcm . N-type ingots without impurities but with low resistivity, as well as with individual impurities and normal resistivity have been made but have not yet been analysed.

Ingot code and impurity concentrations in feedstock are given in Table 1. Note the distinct difference between impurity level in feedstock versus in ingot or wafer. The ppm-levels in feedstock are reduced to ppb or less in the ingot, due to segregation.

2.2 Cell process

The p-type cell process was a standard industrial process: alkaline saw-damage etch, phosphorous diffusion in an IR belt furnace, remote plasma-enhanced CVD of a SiNx front surface coating, screen printed metallisation, and co-firing. For the experiments in this abstract, the typical cell efficiency with this process on good quality wafers was 14.5-15.0%.

The n-type cell process was an early version of the cell process developed in the NESSI project [11]. It is mostly based on industrial process steps: alkaline saw-damage etch, boron diffusion in a quartz tube furnace, remote plasma-enhanced CVD of a SiNx front surface coating, screen printed metallisation, and co-firing. For the experiments in this paper, the typical cell efficiency with this process on good quality wafers was 12.5%. One of the aspects limiting the cell efficiency is the absence of surface passivation of the boron emitter by the SiNx coating. The cell size was typically (100mm)², in some cases (125mm)².

As reference for the experimental ingots, conventional mc-Si ingots were used. For the p-type cells, several regular mc-Si ingots were used. For the n-type ingots, reference mc-Si wafers from several experimental n-type ingots were supplied by Deutsche Solar [11].

2.3 Results

The resistivity profiles of the p-type ingots are relatively flat because boron hardly segregates ($k_{\text{eff}} \sim 0.8$). Only the Al-contaminated p-type ingot shows some more resistivity variation due to doping by Al with segregation coefficient $k_{\text{eff}} \sim 0.007$. The resistivity in the n-type ingots also follows a profile in approximate agreement with Al-segregation. This is consistent with the fact that while phosphorous dominates the type of doping, Al segregation dominates the change of resistivity through the ingot.

In ingots n-5Al1Ti3Fe and n-40Al10Ti70Fe the Al and P-concentrations were measured by chemical analysis. The resistivity is higher by a factor 2 (n-5Al1Ti3Fe) to 3 (n-40Al10Ti70Fe) than expected from the chemical dopant concentration. Most likely this indicates a reduced carrier mobility in these ingots (due to the other impurities).

The main parameter in our interpretation of the results is the carrier diffusion length derived from the internal quantum efficiency of the cells. This is an appropriate parameter to study the impact of the metallic impurities, since it removes many variables such as reflectance, front surface and emitter recombination, which would otherwise obscure the results.

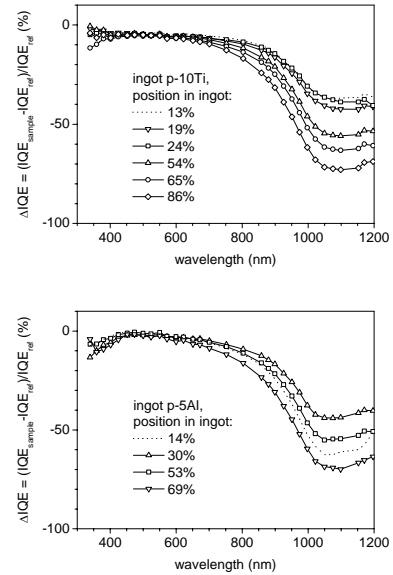


Figure 1: Internal quantum efficiency (presented as deviation in % from average of commercial reference material) for the p-type ingots doped with Ti and Al.

Fig. 1 shows typical examples of the internal quantum efficiency for some of the p-type ingots. The suppression of IQE at long wavelengths is due to the metallic contaminants in the experimental ingots. The suppression in Fig. 1 corresponds to a reduction of cell efficiency of approx. 15%_{relative} in the bottom of the ingot, and 20-25%_{relative} at 80% of ingot height.

Fig. 2 shows the carrier diffusion length and lifetime, derived from the internal quantum efficiency for all investigated ingots.

The suppression of IQE in p-10Ti and p-10Ti16Fe is similar. One could therefore conclude that the suppression is largely due to the Ti present in these ingots, rather than the Fe present additionally in p-10Ti16Fe. However, this conclusion is probably only partly true and we will consider the uncertainty in this statement in section 2.6.

We have observed a slight degradation of cell efficiency (by a few percent relative) due to carbon added to the feedstock. This may have to do with impurities present in the carbon doping material. Surprisingly, we have not observed significant degradation of cell fill factor by this carbon doping, even by doping up to 50 ppmw of carbon [10]. However, the number of cells we have processed was limited, and the fill factor of all cells was rather low and varying, so this will have to be studied more carefully, with better statistics.

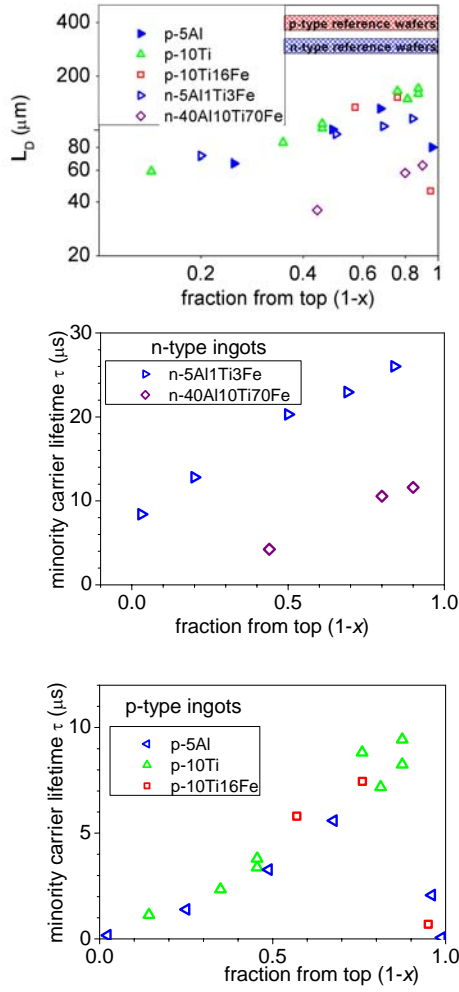


Figure 2: Minority carrier diffusion length (from Basore-fit of IQE) and corresponding minority carrier lifetime. For the conversion from diffusion length to lifetime, the additional suppression of carrier diffusion in the n-type ingots by a factor 2-3 was taken into account.

2.4 Modelling of results for Al and Ti

In the Shockley-Read-Hall recombination model, the recombination lifetime scales inversely with the concentration of a defect. In a simple assumption therefore, changing the impurity concentration C in the feedstock would change the carrier lifetime τ_{eff} in the cell as

$$1/L_{\text{eff}}^2 \propto 1/\tau_{\text{eff}} \propto C \quad (1)$$

Using this assumption, the dependence of cell efficiency on feedstock contamination can be modelled with, for example, PC1D.

However, in reality, a change of the impurity concentration could change all sorts of interactions (with the crystallisation process, crystal defects, other impurities, etc.) so that this scaling might be lost. Our experiments allow us to verify whether scaling (1) holds, because:

- In each ingot there is a range of impurity concentration, increasing from bottom to top due to segregation.
- The bulk recombination lifetime in the cell can be derived from a Basore-fit ($1/\text{IQE}$ versus $1/\alpha(\lambda)$) of the infrared part of the internal quantum efficiencies.

The basis of our analysis is the Scheil equation for segregation [12]:

$$C_S = k_{\text{eff}} C_0 (1 - f_s)^{k_{\text{eff}} - 1}$$

where C_0 is the initial concentration in the liquid silicon and f_s the solidified fraction. k_{eff} is the segregation coefficient, normally $k_{\text{eff}} \ll 1$. The concentration of impurities incorporated into the solid phase C_S during crystallization is given by $C_S = k_{\text{eff}} C_L$.

Fig. 3 shows the Al-concentration in ingot S6, derived from the difference of resistivity between S6 and the other ingots. It follows the Scheil equation with $k_{\text{eff}} = 0.007$. Fig. 4 shows that also $1/\tau_{\text{eff}}$ (or equivalently, $1/L_{\text{eff}}^2$) follows the Scheil equation. This is a strong indication that scaling as discussed above is valid, for both ingots p-5Al and p-10Ti. It may be assumed that extrapolation of such scaling to lower impurity concentrations is then also allowed.

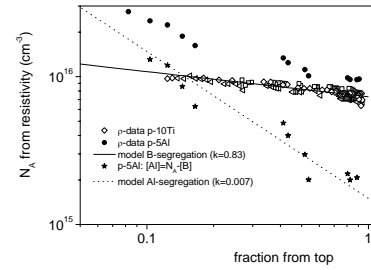


Figure 3: Comparison of excess acceptor concentration in p-5Al with Scheil equation (dotted line).

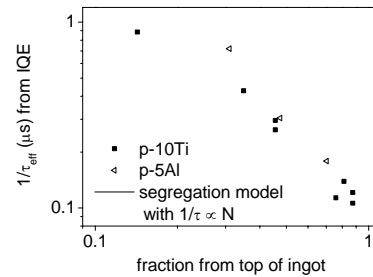


Figure 4: Comparison, for p-5Al and p-10Ti, of $1/\tau_{\text{eff}}$ from IQE with the Scheil equation.

2.5 Cell efficiency versus impurity concentration

Under the assumption of scaling as described by eq. (1), one can model in PC1D the effect of a range of impurity concentrations in feedstock. The results are given in Fig. 5, for a standard industrial cell process, and for an improved 17% efficiency cell process as developed by ECN.

For example, our data for Al and Ti both show approx. 25%_{rel} reduction of $J_{\text{sc}} V_{\text{oc}}$ at a position of 15mm below the top of the ingot. According to Fig. 5, the impurity concentration will have to be reduced by a factor 60 to arrive at 3%_{rel} reduction. This implies a feedstock specification of 0.08 ppmw for Al, or 0.17 ppmw for Ti.

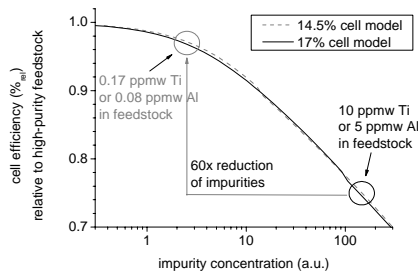


Figure 5: Cell efficiency modelled under assumption of scaling of lifetime degradation in the cell with impurity concentration in feedstock (based on eq. 1, as observed in the experiments). Translation of experimental data to example cell spec of 97%_{rel} is indicated with grey arrow.

2.6 Modelling of results for Fe

Unfortunately, there are no results yet for a mc-Si ingot from feedstock doped *only* with Fe. As mentioned in section 2.3, from the small difference in recombination lifetime in ingots p-10Ti and p-10Ti16Fe, it seems that the impact of Fe is limited. However, this has a high level of uncertainty. Due to the strong effect of Ti, the sensitivity to other contaminants is strongly reduced.

For example, a Ti concentration which results in a reduction of cell efficiency by 20%_{rel}, and a Fe concentration which results in a reduction of cell efficiency by 13%_{rel}, together give an efficiency reduction of 22%_{rel} (20%_{rel} + 13%_{rel} → 22%_{rel}). Since in our experiments the difference between 20%_{rel} and 22%_{rel} is not reliably distinguishable, the effect of the 16 ppmw of Fe by itself could be anything between zero and more than 10%_{rel}.

In fact, when assuming a rather conservative uncertainty of 5%_{rel} in our experiments, the effects of the Fe and Ti in ingot p-10Ti16Fe might even be comparable without showing up as a clear deterioration compared to ingot p-10Ti (20%_{rel} + 20%_{rel} → 25%_{rel}!).

Another question that still has to be answered for Fe is whether the linear scaling according to eq. (1) is valid for that impurity. Deviations from eq. (1) are more likely for mobile impurities, because these can precipitate and be gettered, both of which may be strongly nonlinear phenomena.

2.7 Comparison of p- and n-type ingots

Ingot n-5Al1Ti3Fe and p-5Al are both doped with approx. 5 ppmw of Al but ingot n-5Al1Ti3Fe has approx. 10-30x lower resistivity than ingot p-5Al. Nevertheless, ingot n-5Al1Ti3Fe has significantly higher lifetime than ingot p-5Al. Thus, Al is much less harmful for the recombination lifetime in the n-type ingot. However, due to the lower diffusivity of minority carriers in the n-type silicon, the difference in *diffusion length* in these two ingots is rather small.

Ingot n-40Al10Ti70Fe is doped with an amount of Ti comparable to the p-type ingot p-10Ti, and additionally has a large amount of Al and Fe, and a resistivity approx. 10x lower than the p-type ingots. Nevertheless, the carrier lifetime is similar to the p-type ingots with 10 ppmw of Ti, and only a factor 3 lower than ingot n-5Al1Ti3Fe. Due to the different minority carrier diffusivities, the *diffusion length* in ingot n-40Al10Ti70Fe is smaller than in the p-type ingots doped with 10 ppmw of Ti.

Thus, we observed favorable effects due to the n-type doping. The studied metal impurities have lower impact on carrier lifetime in the n-type doped wafers than in the p-type doped wafers. However, the results for carrier diffusion length are less clearly favoring n-type.

2.8 Ingot resistivity and V_{oc}

An advantage of low resistivity n-type wafers can be that it increases the open circuit voltage of the cell. Normally (in p-type cells with common impurities such as Fe) a low resistivity causes a decrease of carrier lifetime. Therefore the potential gain in V_{oc} is offset by lifetime-related losses, especially of J_{sc} . A typical optimal resistivity is 1 Ωcm .

In n-type silicon, according to our (preliminary) results, the low resistivity is less harmful for minority carrier lifetime, and the low resistivity may be used to some advantage. As shown in ref [9] the V_{oc} of the contaminated but highly doped wafers from ingot n-40Al10Ti70Fe is even better than the V_{oc} of the uncontaminated but normally doped reference wafers. This is probably why the efficiency of cells from ingot n-40Al10Ti70Fe, relative to the reference cells, is high, similar to that of the p-type ingots doped with 10 ppmw Ti, despite the lower diffusion length.

However, it should be noted that this remarkable effect in V_{oc} was not always observed and appears to depend on cell process conditions.

3 EXTENDED DEFECTS

3.1 Lifetime and defect maps

From a theoretical point of view, it is clear why many *point* defects (especially interstitial ones) are less harmful in n-type silicon than in p-type silicon [7]. However, the cell efficiency of mc-Si cells is often strongly influenced by the presence of *extended* defects. It is therefore relevant to explore and compare the recombination activity of extended defects in p- and n-type silicon.

Defect recombination activity in mc-Si is still a not well understood phenomenon. It has been attributed to precipitates as well as to high concentrations of impurities in strain zones around the defects. In any case, it is believed that the recombination activity of extended defects is at least partly due to precipitates.

Figs. 6 and 7 show the typical response of n- and p-type wafers to gettering and bulk hydrogenation. Qualitatively they are very similar: gettering causes a lifetime improvement inside grains and deterioration of grain boundaries; hydrogenation causes reduction of recombination at the grain boundaries. (the reduction of lifetime inside grains after hydrogenation is probably an artefact related to less effective surface passivation during the lifetime measurement).

It is clear that n-type mc-Si is not free from recombination activity at extended defects. From the similarity of the results in p- and n-type mc-Si it may perhaps be deduced that precipitates, and not just high impurity concentrations in strain zones, account for the recombination (high concentrations of the common impurities in strain zones should follow the properties of point defects and thus be relatively harmless in the n-type Si).

Quantitative and more extensive analysis of results

like Figs. 6 and 7 are however still very much needed..

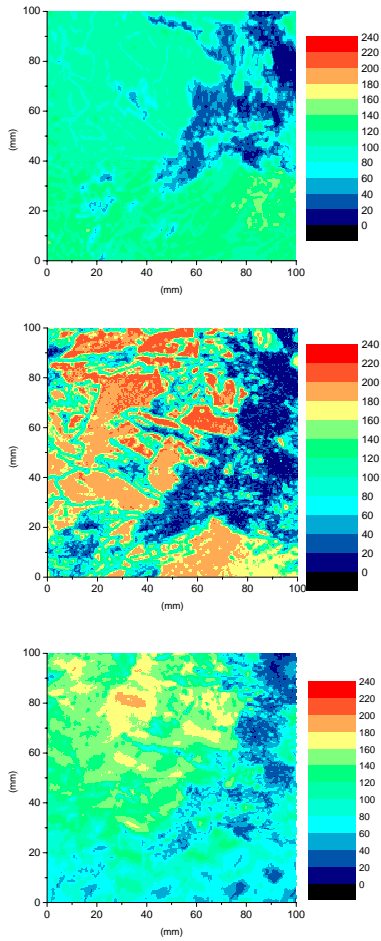


Figure 6: Typical lifetime map evolution of good quality n-type mc-Si from unprocessed (top), via gettered (middle) to gettered and hydrogenated (bottom). Lifetime scales in μs .

3.2 Simple model for precipitate activity

Tan et al. have proposed to relate the recombination activity of precipitates, i.e., the capture cross section, to the Schottky barrier at the interface between precipitate and silicon [13]. Based on this idea, and assuming that the information we have about Schottky barriers on a macroscopic scale also holds for microscopic precipitates, we have considered the implications for the recombination activity in n- versus p-type mc-Si [14]. The results are quite simple: the size of the depletion region around the precipitate determines its capture cross section. Thus, precipitates with higher Schottky barrier are more recombination active. The Schottky barriers between metal silicides and n-type silicon are significantly higher than between metal silicides and p-type silicon [15]. Accordingly, the high Schottky barriers of most silicides to n-type silicon imply a higher capture cross section in such silicon compared to p-type silicon, and therefore *higher* recombination activity in n-type silicon.

The modelling we have done so far applies to isolated precipitates. In reality, the spatial distribution of precipitates may be much more important than the capture cross sections of individual precipitates. Therefore, it is difficult if not impossible to predict the

defect recombination activity. The main conclusion from this simple model about extended defects is therefore that there does not seem to be the same fundamental advantage for n-type Si as there is for point defects.

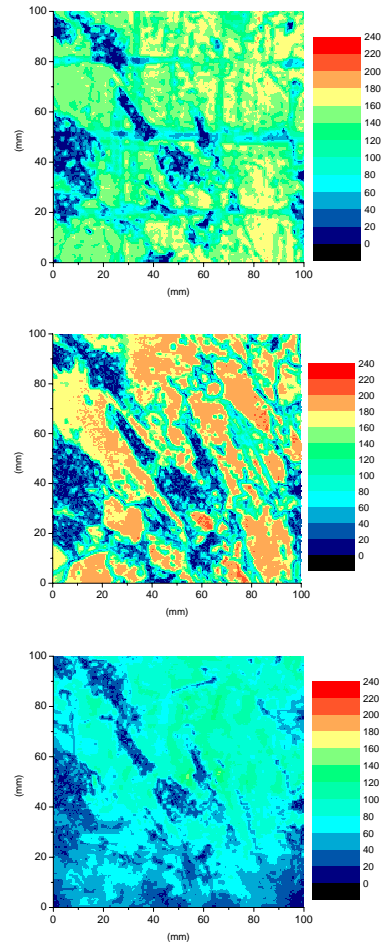


Figure 7: Typical lifetime map evolution of good quality p-type mc-Si from unprocessed (top), via gettered (middle) to gettered and hydrogenated (bottom). Lifetime scales in μs .

4 SUMMARY

In conclusion, we have presented and modeled the effect on mc-Si cell efficiency of certain impurities in silicon feedstock.

Concrete data in p-type ingots was given for:

- reduction of cell efficiency due to Al and Ti,
- evidence for simple modelling of the effect of other concentrations of Al and Ti,
- limited effect of additional 16 ppmw Fe, but with large uncertainty
- high tolerance for high carbon-concentrations, more careful analysis of the carbon effects is however necessary.

Also, the effects of these contaminants were compared experimentally in p-type and n-type doped multicrystalline silicon ingots. We observed favorable effects due to the n-type doping. The studied metal impurities have lower impact on carrier lifetime in the n-type doped wafers than in the p-type doped wafers. The

situation with respect to carrier diffusion length is less clear.

So far, n-type ingots were investigated in which are present, simultaneously, high impurity concentrations as well as high doping levels. The effect of resistivity and the effects of individual impurities should rather be studied separately. This will allow to model and quantify the impact of the impurities in an n-base solar cell as for a p-type base.

Of course, our *results* are to some extent specific for the Crystalox furnace used. However, we expect that our *approach* and the *order of magnitude of results* should be useful for other crystallisation furnaces too.

Finally, we have presented a simple model for recombination activity of precipitates which shows that in that case there does not seem to be the same fundamental advantage for n-type Si as there is for point defects. This is, qualitatively, corroborated by lifetime maps of n- and p-type wafers.

5 ACKNOWLEDGMENTS

We gratefully acknowledge EC Support in projects SOLSILC (ERKG-1999-00005), SISI (COOP-CT-2002-508202), SPURT (NNE5-CRAF-1999-70783), and FOXY (SES6-019811). The content of this paper is the responsibility of the author. The author would like to acknowledge that this work was a collaboration with many colleagues at the project partners of these projects, in particular at Sintef, ECN, ScanArc and Sunergy, University of Konstanz, and Deutsche Solar. He would also like to acknowledge stimulating collaboration with Daniel Macdonald, and very useful discussions with Tonio Buonassisi.

6 REFERENCES

- [1] For impurities in metallurgical silicon see, e.g., Van den Avyle et al., report SAND 2000-0821.
- [2] For impurities in high-purity quartz see, e.g., <http://www.norcryst.no/products2.html>
- [3] L.J. Geerligts et al., 12th workshop on crystalline silicon solar cell materials and processes, Breckenridge, CO, August 12-14th, 2002. p. 216.
- [4] J.R. Davis et al., IEEE Trans. El. Dev. ED-27 (1980) 677.
- [5] J. Fally et al., Revue Phys. Appl. 22 (1987) 529.
- [6] US PV-roadmap.
- [7] D. Macdonald and L.J. Geerligts, Appl. Phys. Lett. **85**, 4061 (2004).
- [8] J. Schmidt, Appl. Phys. Lett. **82**, 2178 (2003).
- [9] L.J. Geerligts et al, Proceedings of the 20th European PV conference, Barcelona, p. 619 (2005); and 21st European PVSEC, Dresden, 2006..
- [10] e.g., T. Buonassisi, this conference.
- [11] J. Libal et al., Proceedings of the 20th European PV conference, Barcelona, p. 793 (2005). T. Buck et al., L.J. Geerligts et al., 21st European PVSEC, Dresden, 2006.
- [12] E. Scheil, Z. Metallk. **34**, 70 (1942).
- [13] T.Y. Tan, and P.S. Plekhanov, Mat. Res. Soc. Symp. Proc. Vol. 669 (2001).
- [14] L.J. Geerligts, unpublished

- [15] Properties of Metal Silicides, eds. K. Maex and M. Van Rossum, Inspec (1995).